Characterization of sequences and mechanisms through which ISE/ISS-3 regulates FGFR2 splicing

Ruben H. Hovhannisyan[1], Claude C. Warzecha[2] and Russ P. Carstens[1,2,*]

[1]Department of Medicine and [2]Cell and Molecular Biology Graduate Group, University of Pennsylvania School of Medicine, 700 Clinical Research Building, 415 Curie Blvd., Philadelphia, PA 19104, USA

ABSTRACT

Alternative splicing of fibroblast growth factor receptor-2 (FGFR2) mutually exclusive exons IIIb and IIIc results in highly cell-type-specific expression of functionally distinct receptors, FGFR2-IIIb and FGFR2-IIIc. We previously identified an RNA *cis*-element, ISE/ISS-3, that enhanced exon IIIb splicing and silenced exon IIIc splicing. Here, we have performed comprehensive mutational analysis to define critical sequence motifs within this element that independently either enhance splicing of upstream exons or repress splicing of downstream exons. Such analysis included use of a novel fluorescence-based splicing reporter assay that allowed quantitative determination of relative functional activity of ISE/ISS-3 mutants using flow cytometric analysis of live cells. We determined that specific sequences within this element that mediate splicing enhancement also mediate splicing repression, depending on their position relative to a regulated exon. Thus, factors that bind the element are likely to be coordinately involved in mediating both aspects of splicing regulation. Exon IIIc silencing is dependent upon a suboptimal branchpoint sequence containing a guanine branchpoint nucleotide. Previous studies of exon IIIc splicing in HeLa nuclear extracts demonstrated that this guanine branchsite primarily impaired the second step of splicing suggesting that ISE/ISS-3 may block exon IIIc inclusion at this step. However, results presented here that include use of newly developed *in vitro* splicing assays of FGFR2 using extracts from a cell line expressing FGFR2-IIIb strongly suggest that cell-type-specific silencing of exon IIIc occurs at or prior to the first step of splicing.

INTRODUCTION

Alternative splicing represents an important mechanism used by the cell to generate multiple transcripts from a single gene and at least 60% of genes appear to generate more than one spliced mRNA (1–3). Despite growing appreciation of the relevance of alternative splicing to normal development as well as its role in disease, the molecular mechanisms that control this process in mammalian cells are poorly understood. A general model of splicing regulation has emerged whereby splicing regulatory factors influence the ability of the basal splicing machinery to recognize consensus sequence elements present at exon/intron (the 5′ splice site) and intron/exon boundaries (the 3′ splice site) (1,4). The 3′ splice site consists of an invariant AG at the end of the intron and a polypyrimidine tract (PPT) located upstream from it. Upstream of the PPT is the branchpoint sequence (BPS) that is also involved in recognition of the 3′ splice site. Together, these consensus sequences are required for recruitment of the spliceosome, the macromolecular machine that performs the catalytic steps of splicing (5). The spliceosome consists of five small nuclear ribonucleoprotein particles, U1, U2, U4, U5 and U6, which, together with numerous additional constitutive splicing factors, assemble in a stepwise fashion at the splice sites. The initial steps include binding of U1 at the 5′ splice site, U2-auxiliary factor 65 and 35 kDa subunits (U2AF65 and U2AF35) to the PPT and 3′ splice site, and splicing factor 1/branchpoint bridging protein (SF1/mBBP) to the branchpoint. Subsequently, U2 is recruited to the branchpoint, followed by addition of U4, U5 and U6. After several structural rearrangements, the two catalytic steps of splicing are carried out. In the first catalytic step, a branchpoint nucleotide (usually adenine) carries out a nucleophilic attack at the 5′ end of the intron to yield a branch structure containing a 2′–5′ phosphodiester bond between the branchpoint nucleotide and the guanine residue at the 5′ end of the intron. In the second catalytic step, the upstream exon is ligated to the 3′ exon with release of the intron as a branched intron. For both constitutive and alternatively spliced exons and introns, the degree to which the splice sites match the consensus sequences determines

their ability to be recognized and spliced. Thus, the splice sites (including the BPS) are often described as being 'strong' or 'weak' depending on their conformity to the consensus, which is presumed to reflect their inherent ability to recruit the spliceosome.

In addition to the splice site consensus sequences, the pattern of splicing is further influenced by auxiliary *cis*-elements referred to as exonic or intronic splicing enhancers (ESEs or ISEs) and exonic or intronic splicing silencers (ESSs or ISSs). The exonic elements (ESEs and ESSs) have been shown to play a significant role in the splicing of both constitutively and alternatively spliced exons (6). In contrast, while intronic elements (ISEs and ISSs) have been shown to influence the splicing of some constitutive exons, they have predominantly been described in regulation of alternatively spliced exons (7). The important role that intronic sequences play in alternative splicing is further highlighted by the fact that intron sequences flanking alternatively spliced exons (exclusive of the splice sites) are more highly conserved phylogenetically than those flanking constitutively spliced exons (8,9). The functions of many auxiliary *cis*-elements are mediated by splicing regulatory proteins that bind these elements and facilitate or prevent splicing at nearby splice sites. Thus, strong phylogenetic conservation of intronic sequences flanking alternative exons is presumed to reflect sequence-specific binding of regulatory factors that are involved in conserved alternative splicing events. Frequently, multiple auxiliary *cis*-elements are present within or flanking alternatively spliced exons and positively or negatively influence splice site recognition. Such observations have led to models of combinatorial control whereby the splicing outcome is determined by the net activity of several splicing regulatory factors that bind these elements (1,10).

We have been studying the mechanisms that lead to cell-type-specific splicing of two mutually exclusive exons, IIIb and IIIc, in the fibroblast growth factor receptor-2 (FGFR2) transcript (Figure 1A). These exons encode two different peptide sequences in the extracellular portion of the receptor yielding two different isoforms, FGFR2-IIIb and FGFR2-IIIc, with distinctly different ligand binding preferences. Expression of FGFR2-IIIb is generally restricted to epithelial cells and FGFR2-IIIc to mesenchymal cells and disruption of the cell-type-specific splicing pattern of FGFR2 has been implicated as one event that can play a role in cancer progression, including prostate cancer (11–13). Previous studies by our laboratory and others have identified several auxiliary
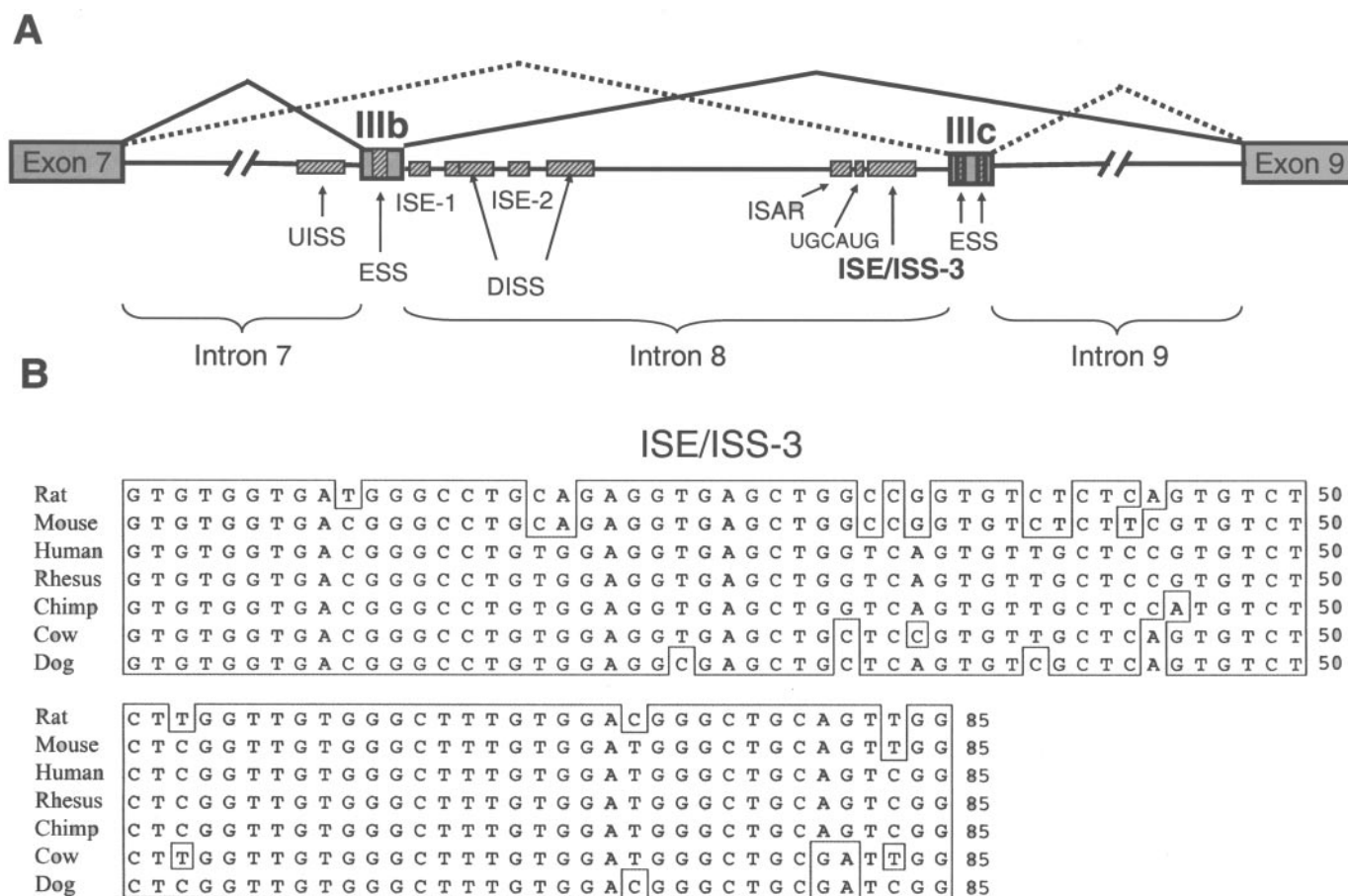

Figure 1. Multiple auxiliary *cis*-elements regulate splicing of FGFR2 mutually exclusive exons IIIb and IIIc. (**A**) Schematic representation of the pre-mRNA in the region containing exons IIIb and IIIc. Exons are indicated by shaded boxes and auxiliary *cis*-elements by hatched boxes. UISS and DISS indicate upstream and downstream intronic splicing silencers, respectively. ESE, exonic splicing silencer. ISE, intronic splicing enhancer. ISAR, intronic splicing activator and repressor. *UGCAUG*, sequence motif that also functions as an ISE for exon IIIb. The locations of FGFR2 introns 7, 8 and 9 are indicated by brackets. (**B**) Alignment of ISE/ISS-3 sequences from the indicated mammalian FGFR2 genes.

cis-elements that can positively or negatively influence inclusion of either exon IIIb or IIIc and are summarized in Figure 1A. While RNA binding proteins that interact with several of these elements have been identified, these proteins have not revealed cell-type-specific differences in expression between cells that include exon IIIb or exon IIIc and thus the mechanism by which cell-type-specific splicing is achieved remains unclear (14–18). We recently identified ISE/ISS-3 (Intronic Splicing Enhancer/Intronic Splicing Silencer-3), so named because its deletion led to loss of cell-type-specific enhancement of exon IIIb as well as loss of exon IIIc repression in cells that express FGFR2-IIIb (19). However, it remained unclear whether the ISE and ISS activities we described were carried out by distinct sequences within the element, or whether the same sequences are involved in both activities. Through systematic mutational analysis of ISS/ISE-3 we have now determined that sequences that are critical for activation of an upstream exon are also involved in silencing of a downstream exon.

We previously demonstrated that the ability of ISE/ISS-3 to silence exon IIIc was facilitated by a highly atypical use of guanine as the primary branch nucleotide. Because guanine as a branch nucleotide was shown to impair the second step of splicing more than the first step of splicing in HeLa nuclear extracts, we previously hypothesized that exon IIIc silencing may be regulated at the second catalytic step. However, using a newly developed *in vitro* splicing system from a cell type that expresses FGFR2-IIIb, we show here that the ability of different branch nucleotides to carry out exon IIIc splicing *in vivo* correlates with their efficiency in carrying out the first step of splicing *in vitro*. Furthermore, cell-type-specific exon IIIc silencing does not absolutely require a guanine as the branch nucleotide as a consensus BPS containing adenine as the branch nucleotide can also result in exon IIIc silencing when accompanied by detrimental PPT mutations. Therefore, exon IIIc silencing involving ISE/ISS-3 prevents use of its associated 3′ splice site at or prior to the first step of splicing.

MATERIALS AND METHODS

Plasmid construction

All minigenes were made using standard cloning techniques. pI-11-FS-CXS, pI-11-FS-CXS-IIIb Mut, pI-XN-33.51-IF5, pI-11-FS and pI-11(-H3)PL-3CT constructs were described previously (19). The ISE/ISS-3 fragment presented in Figure 2B and C and Figure 4 was a 105 nt insert obtained by PCR of pI-11-FS with ISE3-Cla-F2 (5′-CATCGATGTGT-GGTGATGGGCCTGCAG-3′) and ISE3-Xho-R4 (5′-CTCG-AGGTGCTGGCCATCAGGAGATT-3′) primers and insertion into the ClaI/XhoI sites of the indicated minigenes. The ISE/ISS-3 element presented in all other figures consisting of the 85 nt sequence element shown in Figure 2A was made by PCR amplification of pI-11-FS with primers ISE-3-Cla-F2 and ISE3-Xho-R5 (5′-CTCGAGCCAACTGCAGCCCGTCCAC-A-3′). The difference between these inserts is a non-functional 20 nt at the 3′ end of the 105 nt element. All ISE/ISS-3 mutations and the PPT mutations were introduced using PCR-based oligonucleotide-mediated mutagenesis. The control BG fragment (105 nt) was obtained by PCR of the second intron of human β-globin gene with BG-105-F (5′-CCGGGCGGCCGCTATACTTAATGCCTTAACAT-3′) and BG-105-R (5′-CCGCATCGATGATTGTAGCTGCTAT-TAGCA-3′) primers. The control BS fragment (85 nt) was made by PCR of pBlueScript (Stratagene) with primers BS85-Cla-F (5′-CATCGATTCTACACGACGGGGAGTC-AG-3′) and BS85-Xho-R (5′-CTCGAGTACCAATGCTTAA-TCAGTGA-3′). To generate the fluorescent minigene PKC-neg-33.51-IF-5-EGFP we first modified pIRESneo3 (Clontech) by removing the synthetic intron. A sequence containing a 5′ exon derived from the rat protein kinase C-γ subunit coding sequence, an adenoviral intron from pI-11 (20), and a 5′ exon derived from the coding sequence of EGFP was then inserted into the NheI and NotI sites in the modified pIRESneo3 vector to generate PKC-neg-EGFP. The enhanced green fluorescent protein (EGFP) sequence was modified by replacing the ATG at the 5′ end of the coding sequence with ATC, and a linker sequence 5′-GCTTAAT-TAAT-3′ was inserted between this substituted codon and the 3′ splice site of the upstream intron. PKC-neg-33.51-IF-5-EGFP was then generated by inserting the 33.51 exon and flanking intron sequences in the BamH1 and XhoI sites in the intron of PKC-neg-EGFP (further details available on request). Derivative plasmids shown in Figure 3 were generated by inserting ISE/ISS-3 or mutant controls between the ClaI and XhoI sites. pI-11(-H3)-Δ1, pI-11(-H3)-Δ2, pI-11(-H3)-Δ3 and pI-11(-H3)-Δ4 minigenes were made by first using PCR of pI-11-FS-CXS with forward primers Intron-2F (5′-CCGGACTAGTCAACGTTTTTGTGTTTGTGT-3′), IAS2-F-Spe (5′-ACTAGTTGGCCATGGAAAAATGCC-CA-3′), 3Cplus-F-Spe (5′-ACTAGTTGTGGGCTGATT-TTTCCATG-3′) and 3Cminus-F-Spe (5′-ACTAGTATCGA-TGTGTGGTGATGGGC-3′), respectively, and the reverse primer Int-3CR-Sal (5′-GTCGACGGTCGGAAATCATTC-GAAAC-3′) followed by cloning into the XbaI and XhoI sites of pI-11(-H3)-PL (19). ISE/ISS-3, Mut 13 and BG were subsequently inserted into the ClaI/XhoI sites of the respective minigenes as shown in Figure 4. The branchpoint mutations were introduced using the QuikChange Kit (Stratagene). All plasmid constructs were prepared with Qiagen MidiPrep kits. Sequences of all the minigenes described were confirmed by sequence analysis by the University of Pennsylvania Sequencing Facility.

Transfections, RNA purification and splicing analysis

Transfection of DT3 and AT3 cells, RNA purification and RT–PCR analysis of minigene splicing were performed as described previously (19). Data quantification was performed using a Molecular Dynamics PhosphorImager. Flow Cytometry was performed using a Becton Dickinson FACSCalibur and analyzed with BD CellQuest Pro.

Extract preparation and *in vitro* splicing assays

HeLa and KATO III nuclear extracts were prepared as described previously (21). KATO III cells were grown by the National Cell Culture Center (Minneapolis, MN) and shipped overnight on wet ice prior to extract preparation. *In vitro* transcription of pre-mRNAs and *in vitro* splicing was performed as described previously (19).
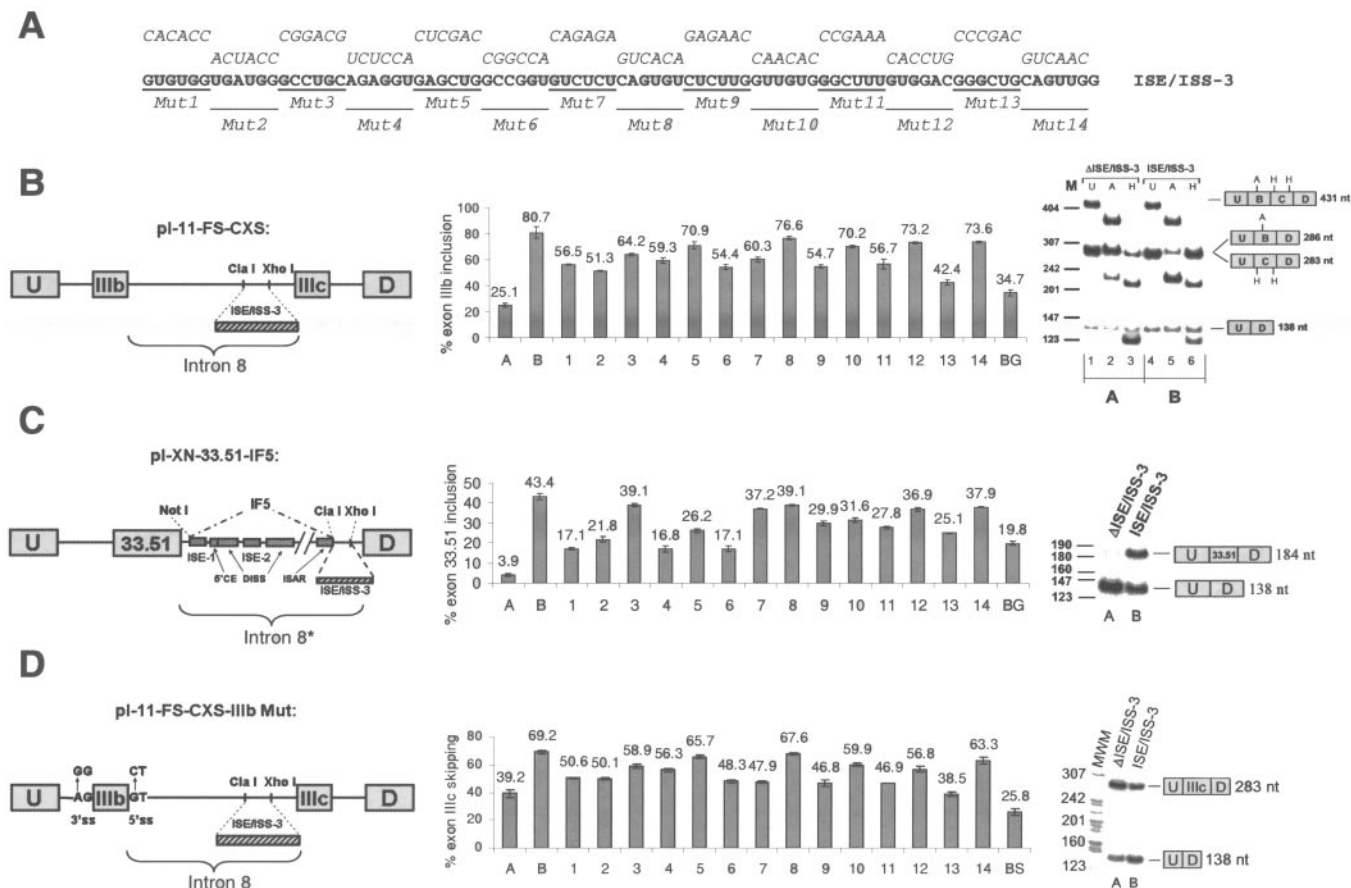
Figure 2. Systematic mutational analysis of ISE/ISS-3 defines sequences that are critical for its function as an ISE and ISS. (**A**) The wild-type ISE/ISS sequence is indicated and 14 separate mutations are indicated above in italics and numbered as indicated below the wild-type sequence. The wild-type and mutated ISE/ISS-3 sequences (or unrelated control BG or BS sequences) were cloned between ClaI and XhoI sites in the minigenes shown in B, C and D and the resulting minigenes were stably transfected in DT3 cells. (**B**) Results of the mutations on exon IIIb and IIIc splicing in the pI-11-FS-CXS minigene. 'A' indicated minigenes without ISE/ISS-3 and 'B' indicates minigenes with wild-type ISE/ISS-3 inserted and actual RT–PCR results for these minigenes are shown at far right (these same designations apply to C and D). The graph represents percentage of spliced minigene products containing exon IIIb. Determination of products containing exon IIIb or exon IIIc was determined by digestion of the RT–PCR products with endonucleases AvaI or HincII, which digest products containing exon IIIb and IIIc, respectively. Exon IIIb inclusion is therefore calculated as the amount of RT–PCR product remaining after HincII digestion divided by the sum of that remaining after both AvaI and HincII digestion. U(above lanes 1 and 4), undigested products; A, AvaI digested products; H, HincII digested products. (Note: we also observe a small fraction of products containing both exons IIIb and IIIc as well as those in which both exons are skipped, but these products are not considered here). (**C**) Results of mutations on inclusion of the upstream exon 33.51 in minigene pI-XN-33.51-IF5. Here an asterisk is used to indicate that a partially truncated sequence derived from intron 8 containing all the shown *cis*-elements was used in the heterologous minigene. A representative RT–PCR is shown at right and the percentage exon 33.51 for all mutations is shown graphically. (**D**) Results of mutations on skipping of exon IIIc in minigene pI-11-FS-CXS-IIIb-Mut. The schematic at left indicates mutations in the 3′ and 5′ splice sites of exon IIIb. BG and BS represent size-matched unrelated control sequences derived from human β-Globin and pBluescript, respectively. U and D in the schematics represent upstream and downstream adenoviral exons present in each minigene. In this and subsequent figures, experiments were performed in triplicate and error bars indicate SD.

RESULTS

Systematic mutational analysis identifies several critical regulatory sequence elements within ISE/ISS-3

We have previously shown that ISE/ISS-3 plays a role in both activation of exon IIIb splicing and silencing of exon IIIc splicing in cell types that express FGFR2-IIIb from its position in the intron (intron 8) located between these mutually exclusive exons (19). Thus, deletion of ISE/ISS-3 independently results in both loss of exon IIIb splicing activation and loss of exon IIIc repression in DT3 cells (that express FGFR2-IIIb). In contrast, deletion of ISE/ISS-3 did not result in any change in AT3 cells (that express FGFR2-IIIc), which maintained exclusive inclusion of exon IIIc. We previously defined a minimal 85 nt sequence that was sufficient to carry out these regulatory

activities. This 85 nt sequence shows extensive phylogenetic sequence conservation consistent with its critical role in splicing regulation (8,9) (Figure 1B). In order to better characterize specific sequences within ISE/ISS-3 that mediate FGFR2 splicing regulation we introduced a series of scanning mutations by sequentially mutating blocks of 6 nt along the length of the element (Figure 2A). Sequences containing the mutations were initially inserted into an FGFR2 minigene, pI-11-FS-CXS, in which ISE/ISS-3 had been deleted and replaced with ClaI and XhoI restriction sites (Figure 2B). This minigene contains both exons IIIb and IIIc as well as all other known regulatory *cis*-elements shown in Figure 1A. Plasmid minigene constructs were generated containing the wild-type ISE/ISS-3 element or ISE/ISS-3 elements containing each of 14 different mutations. These minigenes were transfected
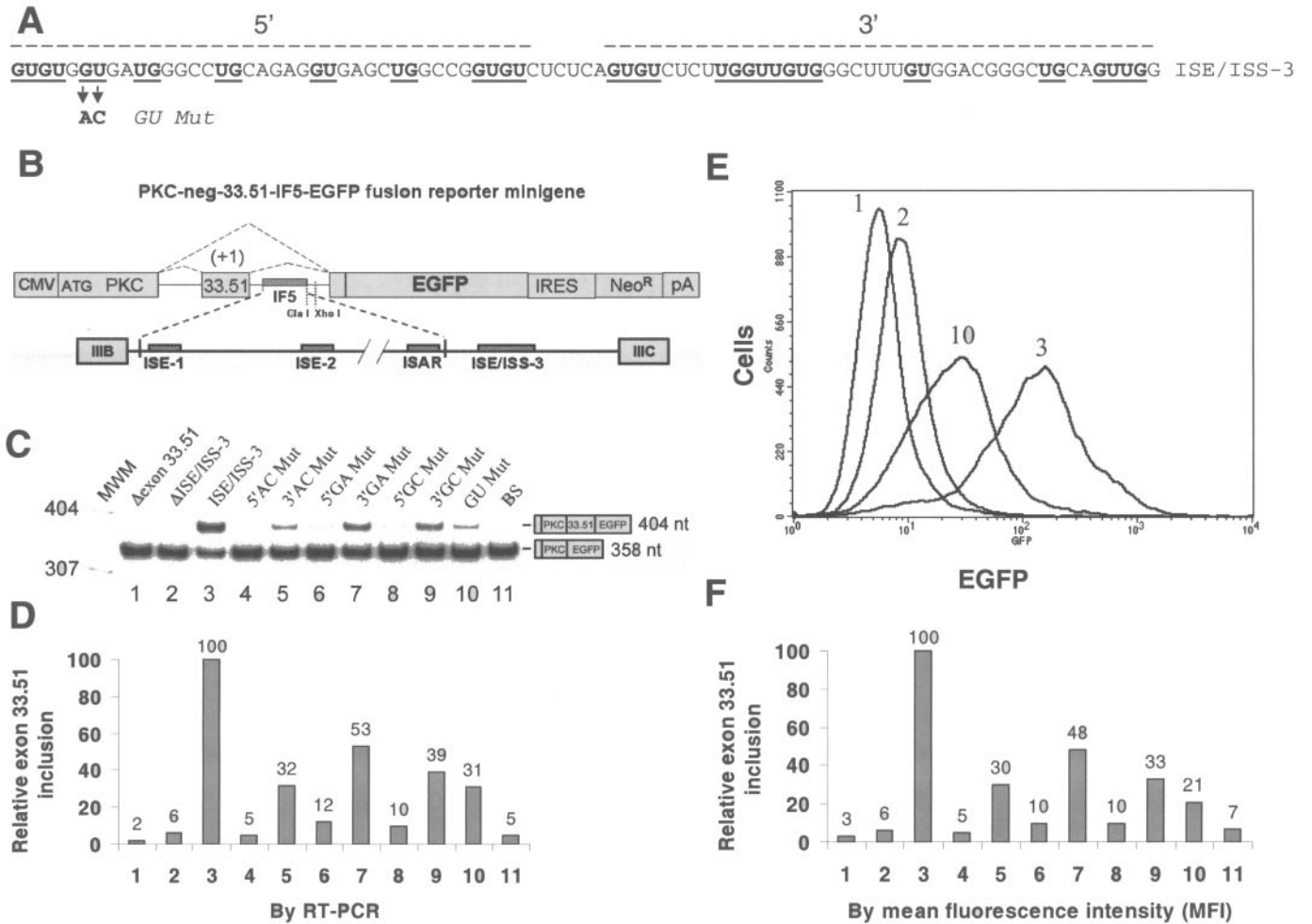
Figure 3. Fluorescent reporter minigenes facilitate identification of GU-rich sequences in the 5′ half of ISE/ISS-3 as most critical for its function. (**A**) ISE/ISS-3 with GU or UG dinucleotides that were mutated in bold and underlined. The 5′ and 3′ sequences are indicated by the dashed line and a single GU to AC mutation is indicated (GU Mut). (**B**) Schematic of the Fluorescent minigene developed for analysis of ISE/ISS-3 function. (**C**) Results of RT–PCR in DT3 cells stably transfected with the respective minigenes. The fluorescent minigene PKC-neg-EGFP containing no internal 33.51 exon (Δ exon 33.51) is shown in lane 1. Lanes 2 and 3 represent results in which ISE/ISS-3 is absent or present downstream of exon 33.51, respectively. Lanes 4–9 indicate minigenes in which the GU or UG dinucleotides have been changed to AC, GA or GC in the 5′ or 3′ half of ISE/ISS-3. GU Mut represents a minigene with the single GU to AC mutation and BS is the size-matched control. The value of 1.1% for lane 1 likely reflects background radioactivity detected by the phosphorimager given the absence of exon 33.51 in the minigene used. (**D**) Graphical presentation of the % exon 33.51 inclusion normalized to the amount of exon inclusion obtained with the wild-type ISE-ISS-3, which was arbitrarily set at 100% to represent its complete activity. The results were then calculated for each minigene as (% exon 33.51 inclusion/% exon 33.51 inclusion with the minigene containing ISE/ISS-3) × 100. The calculated relative values are indicated above each bar. Numbers are the same as the lanes in 'C' and in the graph in 'F'. (**E**) Representative Flow Cytometric Analysis of pools of stably transfected DT3 cells. Numbers correspond to the minigenes indicated used per lane numbers in 'C'. While only four minigenes are presented for clarity, these experiments were performed and analyzed in parallel with all of the minigenes represented in 'F'. (**F**) Graphical presentation of relative % exon 33.51 as calculated using MFI for the same minigenes shown in C and D. Similar to the normalization used in D, results were calculated as (MFI/ MFI with the minigene containing ISE/ISS-3) × 100. The same set of stable transfections was independently repeated with nearly identical results.

into DT3 and AT3 cells and pools of cells stably transfected with the minigenes were used to harvest RNA and the levels of exon IIIb or IIIc splicing were determined using a previously validated RT–PCR assay (see Figure 2B, far right) (19,20,22). As an additional control we also inserted a size-matched sequence derived from a β-globin intron. In the absence of ISE/ISS-3, we noted that only 25% of spliced products contained exon IIIb in DT3 cells; thus, 75% of spliced products instead contained exon IIIc (Figure 2B, lane A). When the wild-type ISE/ISS-3 element is inserted back in its normal position in intron 8, splicing of exon IIIb is restored with 81% of products now splicing exon IIIb in preference to exon IIIc (Figure 2B, lane B). In AT3 cells, there was no difference in

splicing of minigenes containing ISE/ISS-3 or in which it was deleted; they included almost exclusively products containing exon IIIc (data not shown). For these two minigenes, the actual RT–PCR data are shown at far right and data for all mutations are presented graphically in the middle (Figure 2B). Thus, ISE/ISS-3 functions in a cell-type-specific manner to promote splicing of exon IIIb in favor of exon IIIc (19). When the results of the mutations of ISE/ISS-3 on exon IIIb splicing in DT3 cells were analyzed, we noted that seven mutations (Mut 1, Mut 2, Mut 4, Mut 6, Mut 9, Mut 11 and Mut 13) resulted in a >25% reduction in exon IIIb inclusion compared with the wild-type element (Figure 2C). In contrast, the other seven mutations resulted in lesser degrees of impairment
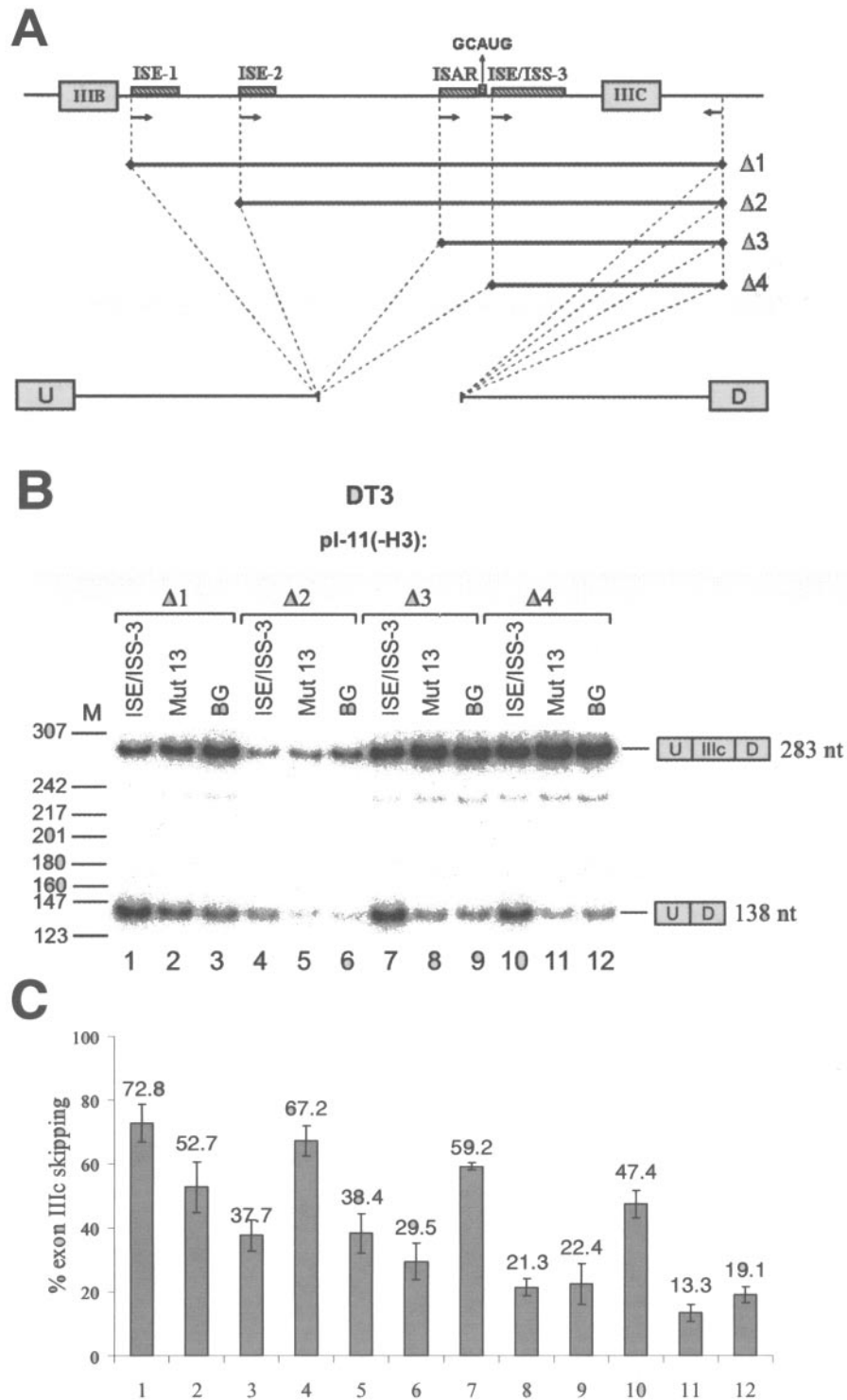
Figure 4. ISE/ISS-3 mediated silencing of exon IIIc does not require upstream intronic sequences. (**A**) Schematic representation of sequences tested for ability to influence exon IIIc skipping. Sequences were amplified by PCR from pI-11-FS-CXS containing either wild-type ISE/ISS-3, mutation 13 (Mut 13) or the control BG sequence. These sequences were then inserted in the intron of an adenoviral splicing construct. (**B**) Results of RT–PCR in DT3 cells stably transfected with the indicated minigenes with successive truncation of intron 8 upstream of ISE/ISS-3. (**C**) Graphical representation of percentage exon IIIc skipping.

in ISE/ISS-3 function. Overall, these results suggested that several sequence motifs along the length of the element are collectively required to mediate the role of ISE/ISS-3 in maintaining FGFR2-IIIb expression. In addition, insertion of the size-matched control BG sequence did not restore exon IIIb splicing, further supporting a conclusion that specific sequences of ISE-ISS-3 are required for FGFR2 splicing regulation.

Sequences within ISE/ISS-3 that mediate splicing activation of an upstream exon also result in splicing repression of a downstream exon

The fact that several of the mutations of ISE/ISS-3 result in a partial switch from exon IIIb to exon IIIc splicing suggested that they disrupt sequences required for exon IIIb activation, exon IIIc repression or both. However, in the minigenes that contain both exons IIIb and IIIc it is not possible to separately examine the effect of each mutation on these two distinct regulatory properties. We previously showed that the entire ISE/ISS-3 element can independently activate exon IIIb as well as repress exon IIIc in DT3 cells (19). However, it remained possible that some sequences within ISE/ISS-3 could activate splicing of the upstream exon IIIb, while other sequences are predominantly involved in repression of the downstream exon IIIc. We therefore tested all of the mutations in contexts in which these activation and repression functions can be independently analyzed. To study activation we used a previously described heterologous minigene, pI-XN-33.51-IF5 in which we inserted ISE/ISS-3 downstream of a troponin exon (exon 33.51) and determined the amount of its inclusion versus skipping (Figure 2C). This heterologous minigene also includes FGFR2 intron 8 *cis*-elements located upstream of ISE/ISS-3 such that the context of its function relative to the regulated exon is similar to that in its endogenous position. To study repression we used a minigene, pI-11-FS-CXS-IIIb-Mut, in which both the 3′ and 5′ splice sites of exon IIIb are mutated to preclude exon IIIb splicing (Figure 2D). We stably transfected DT3 cells with both types of minigenes and determined the degree to which the mutations influenced the ability of ISE/ISS-3 to enhance or silence splicing of an upstream or downstream exon, respectively. To simplify comparison we present the results for exon IIIc repression as the percent of skipping (relative to exon IIIc inclusion) and for activation as the percent troponin exon inclusion (relative to skipping). As shown in Figure 2C and D, it can be seen that the same mutations that caused a switch from exon IIIb to IIIc splicing generally also affected both splicing enhancement of an upstream exon as well as silencing of a downstream exon, although there were some differences in the relative degree to which the different mutations affected each function. These results thus demonstrate that ISE/ISS-3 is a distinct element with dual effects on splicing and thus does not consist of separable elements that independently either activate splicing of an upstream exon or repress splicing of a downstream exon.

GU-rich sequences in the 5′ end of ISE/ISS-3 constitute the most important functional fragment of ISE/ISS-3 as determined using a novel fluorescence-based splicing assay

ISE/ISS-3 has a notably high GU content, with G or U comprising 74% of its nucleotides. We also noted that mutations that impaired splicing regulation were somewhat more prevalent within a highly conserved stretch at the 5′ end of the element containing several GU or UG dinucleotides. We mutated all GU or UG dinucleotides in either the 5′ or 3′ half of ISE/ISS-3 to AC, GA or GC (Figure 3A). These mutations were introduced in a modified version of the heterologous minigene described previously (Figure 2C). In this minigene,

PKC-neg-33.51-IF-5-EGFP, a 5′ terminal exon was substituted that consisted of a 159 nt open reading frame derived from rat protein kinase C (PKC)-γ containing an optimal Kozak consensus sequence at the 5′ end (Figure 3B). A 3′ terminal exon was inserted that contained a coding sequence for EGFP. The intron sequences and the exon 33.51 sequence were unchanged from that of pI-XN-33.51-IF5 (Figure 2C). The design of this minigene established an open reading frame in the 5′ exon that, when exon 33.51 was skipped (or not present as in Δ exon 33.51), did not maintain an open reading frame encoding EGFP. However, inclusion of the 46 nt exon 33.51 was predicted to restore a reading frame encoding an EGFP fusion protein containing the PKC and exon 33.51 encoded amino acids at the 5′ end. In addition, an Internal Ribosome Entry Site (IRES) directing expression of a neomycin selection cassette was present downstream of the EGFP coding sequence. This design ensured that essentially all cells that survived in selective media expressed the minigenes since the minigene and the selectable marker were translated from a single transcript.

Fluorescent minigenes containing wild-type or mutated ISE/ISS-3 were stably transfected in DT3 cells and exon 33.51 inclusion was determined by RT–PCR. We again observed minimal exon 33.51 inclusion in the absence of ISE/ISS-3, but over 50% inclusion when it was present (Figure 3C and D, lanes 2 and 3). We found that mutation of all GU or UG dinucleotides in the 5′ half of the element was sufficient to abolish ISE activity, whereas mutations in the 3′ half only partially impaired its function (Figure 3C and D, lanes 4–9). The fact that three different sequence replacements achieved similar outcomes suggests that the reduction in exon 33.51 inclusion results from loss of sequences in ISE/ISS-3 that are critical for its function and is not due to the unintended introduction of sequences that silence its splicing. Furthermore, these results suggest that the 5′ end of ISE/ISS-3 is required in order to enhance splicing of an upstream exon whereas sequences in the 3′ half of the element contribute, but are less crucial. We also analyzed the same set of stably transfected cells by flow cytometry to determine whether the level of green fluorescence in pooled cells stably expressing the minigene constructs was a reliable indicator of the level of exon 33.51 splicing. Representative flow cytometric analysis using several minigenes is shown in Figure 3E to demonstrate the ability to easily detect increased fluorescence in response to ISE/ISS-3 mediated enhancement of exon 33.51 inclusion. To facilitate comparison of RT–PCR to mean fluorescence intensity (MFI) as a means of determining relative levels exon 33.51 inclusion, we normalized the results for each minigene to that obtained with the minigene containing the wild-type ISE/ISS-3 element. When results from the entire set of minigenes were examined, we observed an excellent correlation between relative MFI by flow cytometric analysis and exon 33.51 inclusion determined by RT–PCR (Figure 3D and F, compare graphs). We observed no significant exon 33.51 inclusion and negligible fluorescence in AT3 cells stably transfected with these same minigenes (data not shown).

We used the same fluorescence-based minigene construct to screen a number of more discrete mutations in ISE/ISS-3 and used flow cytometric analysis to identify several mutations that resulted in the greatest loss of exon 33.51 inclusion.

Among the mutations confirmed by RT–PCR to cause significant impairment in ISE/ISS-3 function was a single substitution of an AC for a GU (Figure 3A, C–F, construct 10, Mut GU). We noted that this mutation occurred within an 8 nt sequence consisting entirely of Gs or Us that was completely conserved among the species examined in Figure 1B, and both mutations involving this region (Mut 1 and Mut 2) impaired splicing regulation. Again, we noted a very tight correlation between exon inclusion relative to the wild-type element as determined by mean fluorescence and RT–PCR.

ISE/ISS-3 can repress exon IIIc splicing independently from upstream intron 8 elements

Previous results from analysis of the intron 8 elements that activate splicing of exon IIIb suggested that the most robust splicing activation involved the concerted action of several elements in addition to ISE/ISS-3, including ISE-1, ISE-2, ISAR and a UGCAUG sequence motif located between ISAR and ISE/ISS-3 (19,23). To determine whether ISE/ISS-3 mediated repression of exon IIIc requires cooperation by these upstream *cis*-elements, we made a series of minigenes in which we sequentially shortened intron 8 upstream of ISE/ISS-3 (Figure 4A). Into each of the resulting minigenes we inserted the wild-type ISE/ISS-3, ISE/ISS-3 with Mut 13 or the unrelated BG control sequence. Results from transfection of this series of minigenes in DT3 cells are shown in Figure 4B. When all upstream elements as well as ISE/ISS-3 are present, 73% of the products skip exon IIIc (Figure 4B, lane 1). However, when ISE/ISS-3 contains mutation 13, exon IIIc skipping is decreased (Figure 4B, lane 2). Complete replacement of ISE/ISS-3 with the BS control sequence results in a greater decrease in exon skipping to 38% (Figure 4B, lane 3). When the sequences upstream of ISE/ISS-3 are progressively deleted in the presence of the wild-type ISE/ISS-3 element a gradual decrease in the amount of exon IIIc skipping was observed (Figure 4B, lanes 4, 7 and 10). However, in each case the ability of ISE/ISS-3 to promote exon IIIc skipping is preserved as evidenced by the fact that exon skipping is significantly decreased when it is mutated or replaced. With minigene construct Δ4, none of the intron 8 sequences upstream of ISE/ISS-3, including the UGCAUG motif, is present, signifying that it can function to silence exon IIIc in their absence. The fact that exon IIIc skipping decreased with progressive truncation of intron 8 from the 5′ end could signify a sequence-dependent contribution from upstream elements on exon IIIc repression. However, this could also represent a non-specific effect due to approximation of the upstream exon to the 3′ splice site of exon IIIc. Nonetheless, in each case the wild-type ISE/ISS-3 sequence was capable of repressing exon IIIc splicing in a sequence-dependent manner. Therefore, we conclude that the ISE/ISS-3 element can repress splicing of the downstream exon IIIc independent of the other intron 8 elements described here. It is noteworthy that the construct used to demonstrate ISE/ISS-3 mediated activation of exon 33.51 splicing does not contain any downstream FGFR2 sequences whereas the Δ4 construct shown here to repress exon IIIc does not contain any upstream FGFR2 sequences. Together, these results effectively preclude the possibility that ISE/ISS-3 functions via an RNA secondary structure with other sequences present in the FGFR2 transcript, as was shown for ISE-2 and ISAR (22).

Therefore, it is assumed that the element is bound by regulatory *trans*-acting factors that play a role in splicing regulation.

Exon IIIc repression in DT3 cells is facilitated by a suboptimal guanine branchpoint nucleotide

We previously mapped the branchpoint nucleotide used during exon IIIc splicing by primer extension and determined that the primary branch nucleotide is a guanine (G) (19). This is the only described example in which a G is used as the primary branch nucleotide during splicing of a mammalian pre-mRNA. We showed that substitution of an adenine (A) in place of the branchsite guanine upstream of exon IIIc abrogated the ability of ISE/ISS-3 to repress exon IIIc splicing in DT3 cells with a switch toward constitutive inclusion of exon IIIc (19). Because G was shown to inhibit the second step of splicing to a greater degree than the first step *in vitro* using HeLa cell nuclear extracts, we hypothesized that repression of exon IIIc splicing might occur during the second step of splicing (19,24). Because cytosine (C) or uracil (U) branchpoints differentially inhibit the first and second step of splicing relative to the preferred A, we sought to provide further evidence for or against this hypothesis by directly comparing the efficiency of exon IIIc repression using all four possible branch nucleotides. The wild-type BPS used, CUAGC, is a perfect match to the minimal mammalian branchpoint consensus, CURAC, with the exception of G in place of the highly preferred A as the primary branch nucleotide (as indicated by the underlined nucleotide). We generated minigenes in which we replaced the G branch nucleotide with A, C or U and assessed their ability to repress exon IIIc in transfected DT3 cells. In the case of both the wild-type G branchpoint as well as when it is substituted with A, we previously confirmed experimentally using *in vitro* splicing assays that the indicated branchpoint nucleotides are indeed the predominant branch nucleophile (19) (data not shown). Thus, we have every reason to believe that this position within the overall BPS element represents the branchpoint nucleotide with each of these substitutions. When A was substituted, exon IIIc was included in over 94% of spliced products (Figure 5B and C, lane 2). For this analysis, we quantified exon IIIc inclusion to include the products containing both exons IIIb and IIIc ('double inclusion') as well as those only including exon IIIc. Products that skip exon IIIc included those that only included exon IIIb or those that skipped both exons. Note that, in contrast to previous figures in which we presented exon IIIc skipping, we will henceforth present levels of exon IIIc inclusion. Relative to use of A as the branch nucleotide, C had previously been shown to be less efficient during the first step of splicing, but the second step of splicing showed no impairment in HeLa nuclear extracts (24). We thus reasoned that if substitution of a C as the branch nucleotide also led to constitutive use of exon IIIc this would be consistent with repression occurring at the second step. However, substitution of a C did not result in constitutive inclusion of exon IIIc, but instead exon IIIc silencing was still achieved, although slightly more inclusion was seen than occurred with G (Figure 5B and C, lane 3). Substitution of U as the branch nucleotide resulted in even lower levels of exon IIIc inclusion than occurred with G even though U was previously shown to be less detrimental for completion of the second step of splicing than G (Figure 5B and C, lane 4) (24).
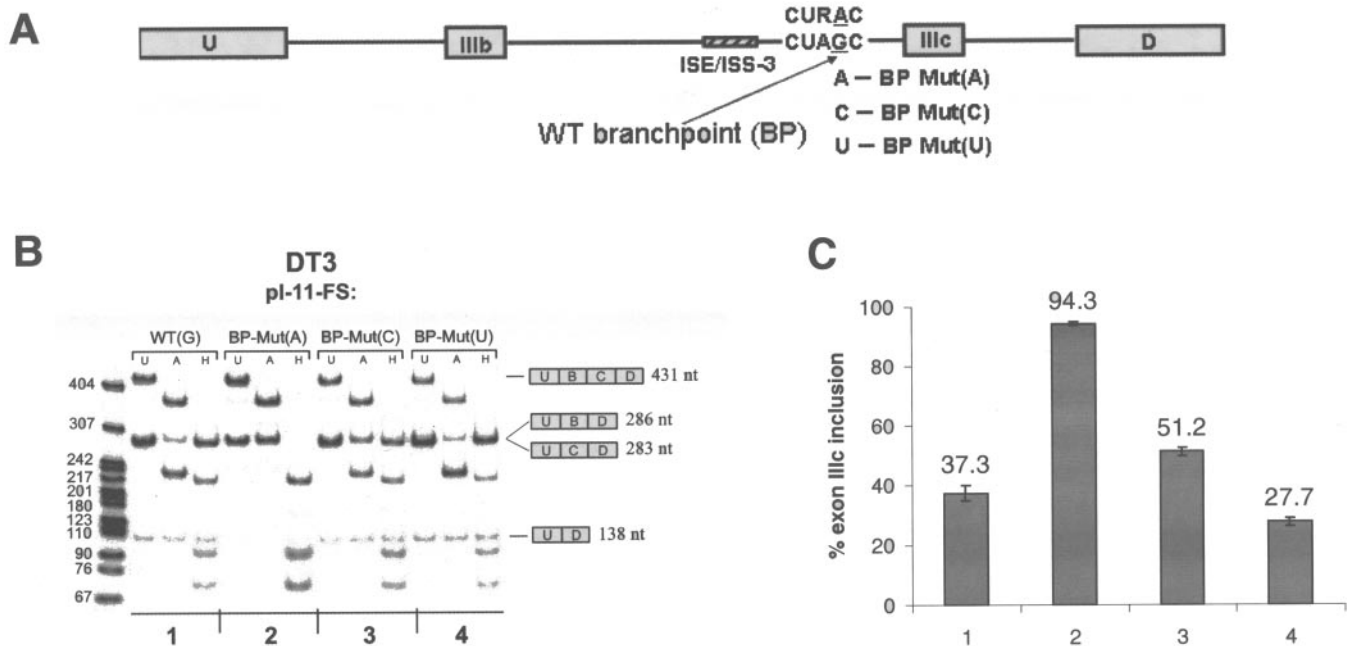
Figure 5. Substitution of an adenine branchsite, but not a cytosine or uracil branchsite, abrogates exon IIIc silencing in DT3 cells. (**A**) Schematic representation of the branchsite substitutions in minigene pI-11-FS. A consensus adenine containing BPS is indicated above the wild-type BPS containing G. (**B**) Results of RT–PCR for minigenes containing each branchsite after stable transfection in DT3 cells. Right, possible splicing products with both IIIb and IIIc exons included (UBCD), with either exon IIIb (UBD) or IIIc (UCD) included and with both exons IIIb and IIIc skipped (UD). (**C**) Graphical representation of the RT–PCR data. The percentage of exon IIIc inclusion is calculated as the percentage of spliced products containing exon IIIc (UCD + UBCD)/(UCD + UBCD + UBD + UD) corrected for molar equivalents.

Therefore, these results *in vivo* were not seemingly consistent with the hypothesis that exon IIIc repression in DT3 cells occurs during the second step of splicing.

The ability to silence exon IIIc with different branchpoint nucleotides correlates with relative efficiency with which the first step of exon IIIc splicing occurs *in vitro* in nuclear extracts from a cell type that expresses FGFR2-IIIb

Previously published relative efficiencies of the two steps of splicing with all four branch nucleotides were determined using pre-mRNA substrates unrelated to those described here (24). Therefore, in order to further assess the effects of the different branch nucleotides in a more relevant context we determined their effects on splicing using pre-mRNAs containing the 3′ splice site of exon IIIc. The pre-mRNA we used contained the same sequences used in construct Δ3 as shown in Figure 4A, but only contained sequences comprising the 5′ half of exon IIIc. Thus, it contained ISE/ISS-3 as well as the entire region encompassing the 3′ splice site of exon IIIc. In addition, we wished to determine the efficiencies of these steps in nuclear extracts from a cell type that expresses FGFR2-IIIb and which therefore would be predicted to repress exon IIIc splicing. We have shown that transfection of our FGFR2 minigenes in HeLa cells results in exclusive exon IIIc splicing as observed in AT3 cells (data not shown), indicating that HeLa extracts would be unlikely to contain factors involved in exon IIIc silencing. Although we were unable to generate splicing competent nuclear extracts from DT3 cells, we have obtained nuclear extracts from the human KATO III cell line that are

competent for *in vitro* splicing. Because KATO III cells express endogenous FGFR2-IIIb and, similar to DT3 cells, splice exon IIIb when transfected with our rat FGFR2 minigenes, extracts from these cells represent a more physiologically relevant system in which to study exon IIIc repression (25) (data not shown). We transcribed pre-mRNAs *in vitro* that contained the wild-type G branch nucleotide as well as A, C and U as was done in the transfected minigenes. *In vitro* splicing reactions were carried out in both HeLa and KATO III nuclear extracts and the efficiency of both steps of splicing was determined (Figure 6). As expected, in extracts from either cell type, both steps of splicing were most efficient when an adenine residue was the branch nucleotide. In HeLa extracts, the first step was nearly as efficient with G or C as the branch nucleotide, and appeared somewhat less efficient with U (Figure 6B and D). However, in KATO III extracts, the first step of splicing was significantly less efficient with either G or C relative to A and U resulted in the greatest impairment (Figure 6C and E). Our observation that the first step of splicing to exon IIIc is least efficient with U as the branch nucleotide contrasts with the previously cited work in which G showed the lowest relative splicing efficiency for both steps (24). Thus, it is clear that there are substrate and/or sequence-context-dependent differences in the degree to which different BPSs affect splicing. The relative rates of the second step of splicing were similar in both cell types with an order of efficiency using each nucleotide being A≥C>U>G. Thus, the efficiency of the first step of exon IIIc splicing in KATO III extracts using each possible branchsite nucleotide correlates directly with the degree to which exon IIIc splicing
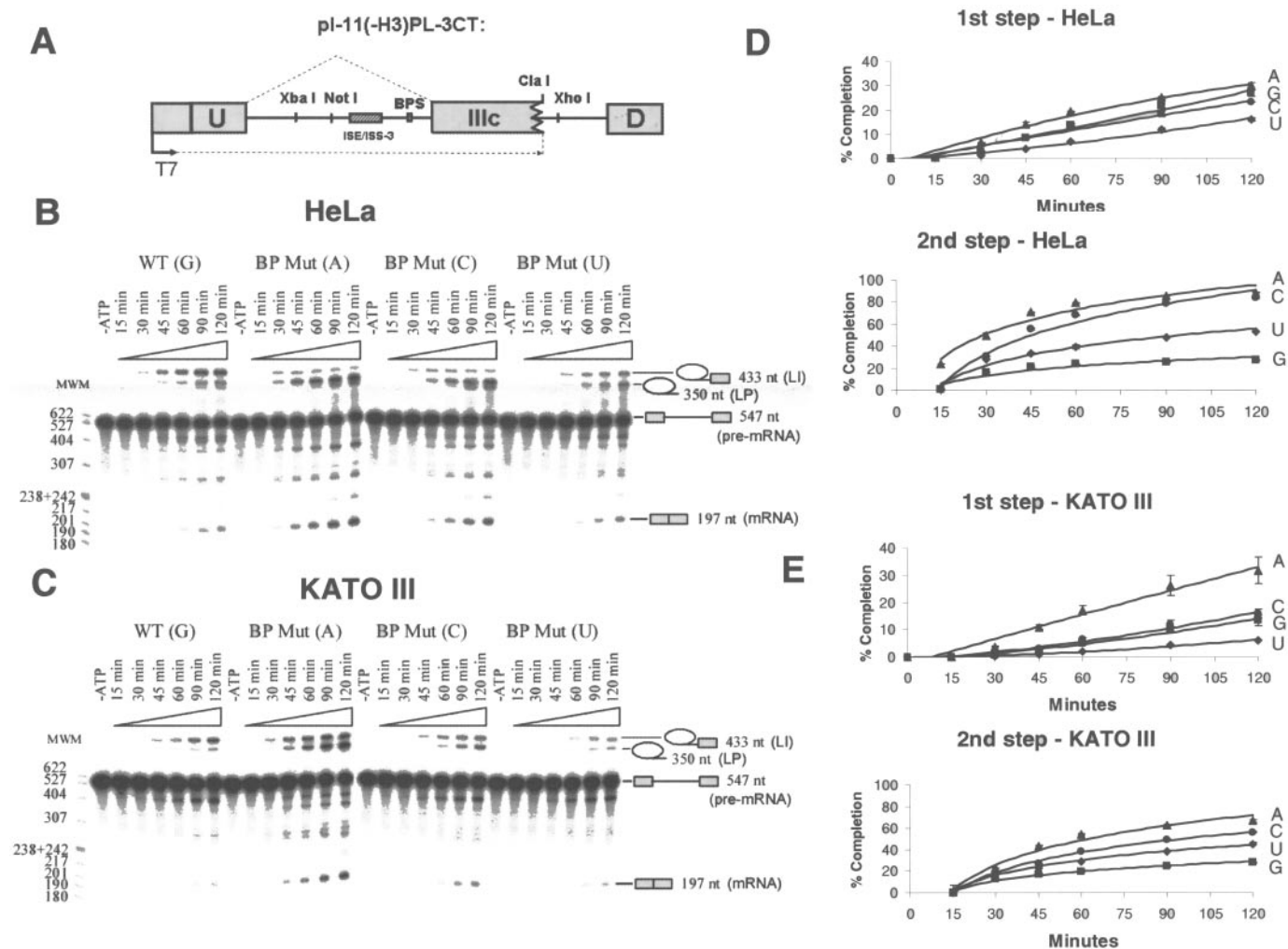
Figure 6. Non-adenine branchsites primarily impair the first step of exon IIIc splicing in KATO III nuclear extracts. (**A**) Schematic representation of the *in vitro* splicing construct. Exon IIIc was truncated and inserted between adenoviral exons together with upstream intron 8 sequences containing ISAR and ISE/ISS-3. *In vitro* transcription with T7 polymerase was carried out after digestion of the plasmid template with ClaI. (**B** and **C**) *In vitro* splicing reactions with HeLa and KATO III nuclear extracts, with pre-mRNAs containing the indicated branch nucleotides. Pre-mRNAs were incubated in nuclear extracts in the absence of ATP ($-$ATP) or with ATP for the indicated time points. At right, icons indicate lariat intermediate (LI), lariat product (LP), pre-messenger RNA (pre-mRNA) and messenger (spliced) RNA (mRNA). (**D** and **E**) Graphical representation of the efficiency of the first or second step of splicing. Calculation of the first step efficiency represents the percentage of pre-mRNA processed to lariat intermediate or lariat product (LI + LP/LI + LP + pre-mRNA). The efficiency of the second step (after step one) represents the percentage of products undergoing the first step that also complete the second step (LI/LI + LP). Results presented in D and E represent experiments performed three times with averages and SD indicated in the graphs. The different branchpoints are indicated as follows: A, triangles; G, squares; C, circles; and U, diamonds.

occurs *in vivo* in DT3 cells. In contrast, whereas G results in the greatest inhibition of the second step, exon IIIc repression in DT3 cells is greater with U than it is with G. These results are most consistent with a mechanism of exon IIIc silencing by inhibition at or prior to the first step of splicing.

Cell-type-specific ISE/ISS-3 mediated repression of exon IIIc in the presence of a consensus BPS can be restored through mutations in the PPT

The highly uncommon use of G as the branch nucleotide suggested that the mechanism of exon IIIc repression may specifically require a weak branchpoint. The fact that substitution of a consensus BPS abolished exon IIIc skipping in DT3 cells is consistent with this possibility. However, it is also noteworthy that the PPT associated with the 3′ splice site

of exon IIIc is very uridine rich, as has been shown to be optimal for selection of a 3′ splice site (26,27). The fact that only 3 G residues interrupt a stretch of 25 pyrimidines in this PPT indicates that it is a 'strong' *cis*-acting determinant of exon IIIc splicing. In fact, numerous studies have indicated that strong PPTs can compensate for weak BPSs, and *vice versa*, suggesting that these two elements collectively contribute to 3′ splice site recognition (28). Thus, if an optimal BPS is combined with the already optimal PPT the combined 'strength' of these signals may preclude exon silencing. To further investigate whether exon IIIc silencing can only occur with a weak branchpoint, we introduced mutations in the PPT of exon IIIc and tested the effects of these mutations on exon IIIc splicing. We substituted 3 guanine residues for 3 U residues in the PPT as shown in Figure 7A. These mutations were introduced in the context of both the wild-type G branchpoint
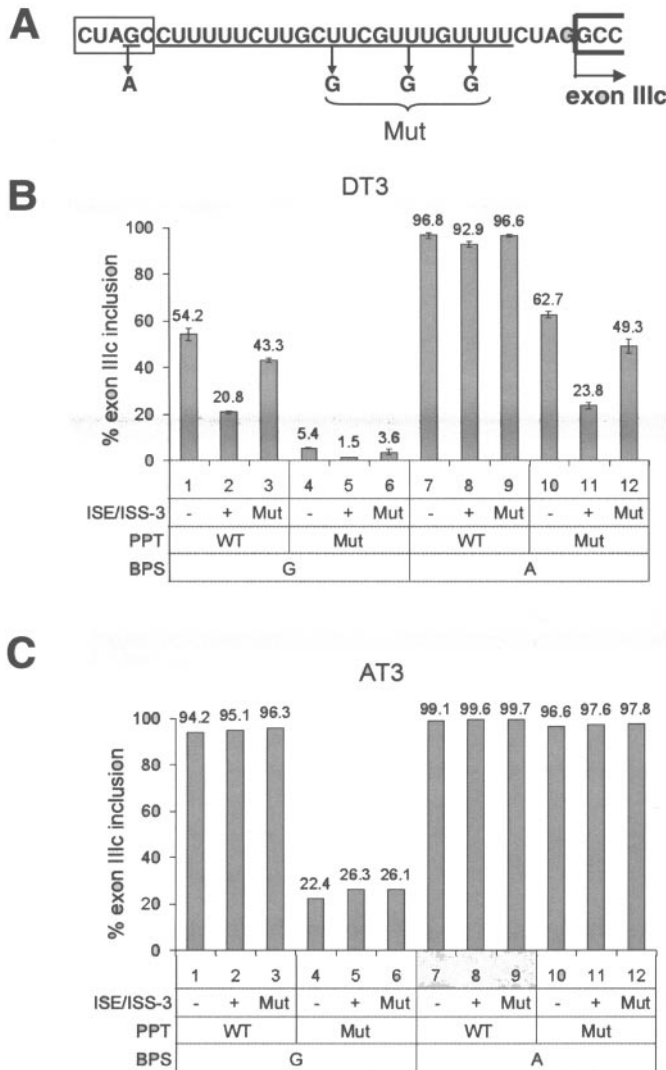
Figure 7. Exon IIIc silencing by ISE/ISS-3 requires either a suboptimal BPS or suboptimal PPT. (**A**) Schematic of the 3′ splice site associated with exon IIIc and the mutations introduced in either the BPS (G to A, indicated by an asterisk) or the PPT (substitution of three Gs in place of U). (**B**) The ability of ISE/ISS-3 to reduce exon IIIc inclusion in DT3 cells as tested in minigenes derived from pI-11-FS-IIIb Mut. Exon IIIc inclusion was determined in the absence (−) or presence(+) of ISE/ISS-3, or with ISE/ISS-3 containing the single GU to AC mutation (Mut) shown in Figure 3 (GU Mut). The effect of ISE/ISS-3 was then further determined with each possible combination involving the wild-type or modified BPS or PPT as indicated. (**C**) Results using the same minigenes transfected in AT3 cells.

and in minigenes containing the optimal adenine branch nucleotide. To simplify the analysis, we introduced these mutations in the context of the pI-11-FS-CXS-IIIb-Mut minigenes to limit the analysis to exon IIIc inclusion. The resulting minigenes, therefore, encompassed a spectrum in which both the BPS and the PPT were 'strong,' either the BPS or the PPT was 'weak,' or in which both were 'weak'. We then further tested each BPS/PPT combination when ISE/ISS-3 was present, deleted or mutated with the single GU to AC mutation described in Figure 3 (GU Mut). Consistent with our previous results, when both the BPS and PPT were 'optimal' we noted nearly constitutive levels of exon IIIc splicing in the presence or absence of wild-type ISE/ISS-3; over 92% exon IIIc

inclusion was achieved in DT3 or AT3 cells, although there was still a slightly decreased level with ISE/ISS-3 in DT3 cells (Figure 7B and C, lanes 7–10). When the wild-type (suboptimal) BPS and wild-type (optimal) PPT were used, ISE/ISS-3 resulted in a >2-fold decrease in exon inclusion in DT3 cells, consistent with previous data (Figure 7B, lanes 1 and 2). The GU to AC mutant resulted in a partial abrogation of the ability of ISE/ISS-3 to repress exon IIIc, similar to its ability to impair exon 33.51 activation (Figure 7B, lane 3). Interestingly, the combination of an optimal BPS and a suboptimal PPT elicited results that were very similar to those with the opposite combination; ISE/ISS-3 caused a >2-fold decrease in exon IIIc inclusion in DT3 cells (Figure 7B, lanes 10 and 11). Furthermore, the relative effect of the GU to AC mutant was nearly identical to that observed with the wild-type BPS and PPT (Figure 7B, lane 12). In AT3 cells, over 90% exon IIIc inclusion was maintained when either the BPS or the PPT was 'suboptimal' regardless of the presence of ISE/ISS-3 (Figure 7C, lanes 1–3 and 10–12). When the BPS and PPT were both suboptimal we noted a dramatic reduction in exon IIIc inclusion in DT3 cells (Figure 7B, lanes 4–6). We nonetheless noted that ISE/ISS-3 could still induce a further decrease in exon IIIc inclusion. Although neither the presence of a suboptimal BPS nor PPT alone was capable of inducing exon IIIc skipping in AT3 cells, the combination of both resulted in predominant exon IIIc skipping (Figure 7C, lanes 4–6). However, in contrast to the results seen in DT3 cells, we noted no measurable difference between the level of skipping in the absence or presence of wild-type ISE/ISS-3. Thus, ISE/ISS-3 can function in a cell-type-specific manner to promote exon IIIc skipping when the 3′ splice site contains either a suboptimal BPS or a suboptimal PPT. Of further note, the fact that mutation of the PPT results in significant impairment of exon IIIc inclusion in AT3 cells that could be rescued by changing the branchpoint G to an A suggests that this is also the branchpoint used *in vivo* in cells that express FGFR2. This is consistent with our previous *in vitro* branchpoint mapping in HeLa cells and suggests that use of an alternative adenine branchsite upstream of this region is unlikely to account for exon IIIc inclusion in cells that express endogenous FGFR2-IIIc.

DISCUSSION

We performed extensive mutational analysis of the ISE/ISS-3 element in order to better understand its role in FGFR2 splicing regulation. The fact that this element displays cell-type-specific splicing regulatory functions only in cells that express FGFR2-IIIb (e.g. DT3 and KATO III cells) suggests that factors that bind this element are centrally involved in the regulation of cell-type-specific splicing of these exons. Our results indicate that GU-rich sequence motifs within ISE/ISS-3 enhance splicing of an upstream exon and repress splicing of a downstream exon and are most consistent with a model in which factors that bind ISE/ISS-3 are involved in both activities and that the primary determinant as to whether the element functions as an enhancer or silencer is its position relative to a regulated exon. Several splicing regulatory factors, including Fox-1, Nova, CELF family members and SR proteins, have been shown to have dual roles as both activators

and repressors of splicing (29–33). In at least a few cases, the ability of these proteins to function either as enhancers or as repressors of splicing was dependent on the position of the corresponding binding site relative to an alternatively spliced exon. Thus, for example, a Nova binding site that functioned as an intronic splicing enhancer downstream of an exon silenced splicing when repositioned within the exon (30). Similarly, Fox-1 binding sites upstream of an ATP synthase G subunit exon mediated exon skipping whereas they mediate exon inclusion when positioned downstream of a fibronectin exon (33). Another recent study showed that intronic AC-rich elements function as either ISEs or ISSs depending on their proximity to a regulated 5′ splice site, an effect likely to be mediated by hnRNP L (34). However, the mechanisms by which these regulators can function to activate or repress splicing remain unclear. The ISE/ISS-3 element is of particular interest as it appears that splicing regulatory protein(s) that bind it can simultaneously achieve such dual roles from a single position in a manner that appears to be determined by its position relative to the regulated exon. While our minigenes containing both exon IIIb and IIIc indicate that these combined activities can occur on the same pre-mRNA, the fact that activation of an upstream exon or repression of a downstream exon by ISE/ISS-3 can occur independently suggests that these activities are not necessarily directly functionally coupled. Using RNA affinity chromatography, we have thus far identified TLS/FUS, KSRP and FBP as proteins that bind the wild-type, but not the 5′ AC mutant, ISE/ISS-3 sequence. However, using co-transfection experiments, we have thus far not been able to demonstrate that any of these proteins alone can promote exon IIIb inclusion or exon IIIc silencing. Therefore, further studies are needed to determine whether additional factors that bind the element are required for its function, or whether post-translational modifications may influence the ability of these proteins to modulate splicing.

Additional mutational analysis was facilitated by the development of a fluorescent splicing reporter assay that allowed us to directly determine the function of ISE/ISS-3 using green fluorescence. Using fluorescent reporter minigenes we initially determined that highly conserved GU-rich sequences in ISE/ISS-3, in particular those in the 5′ end of the element, are essential for its sequence-specific splicing regulatory activity. Using this fluorescent reporter, we screened a set of more discrete mutations in ISE/ISS-3 and using flow cytometry we identified a single GU to AC mutation that significantly impaired its function. Interestingly, we noted an excellent correlation between the MFI in pooled stably transfected cells and the level of inclusion of a heterologous exon as determined by RT–PCR. This feature, whereby fluorescence can directly assay the ability of an intronic element to regulate splicing indicates its potential for broader use in studies of splicing regulation of other transcripts and regulatory elements. Similar to our use here, flow cytometry can be used in conjunction with mutational analysis to characterize other ISEs. Furthermore, a system such as that described here should facilitate systematic identification of sequence motifs that can function as ISEs through screening of randomized sequence libraries. Of note, a recent publication used a fluorescent reporter system and sequence libraries to identify sequences that function as ESSs in living cells and was used to identify conserved motifs that mediate exon skipping (35).

We previously demonstrated that exon IIIc silencing is facilitated by the highly atypical use of a guanine as the primary branch nucleotide and suggested that this may indicate that its silencing is effected during the second step of splicing (19). Although splice site selection is believed to generally be regulated at early steps in spliceosome assembly, the recent demonstration that the Drosophila splicing factor SXL can silence splicing at the second step of splicing *in vitro* has set a precedent for regulation of splicing after the first step (10,36). However, the results presented here argue strongly against this possibility for FRFR2 exon IIIc. We found that the effect of each branchsite nucleotide on exon IIIc inclusion in transfected DT3 cells correlated with the efficiency of the first, but not second, step of splicing in KATO III extracts. Additionally, while the ability of ISE/ISS-3 to repress exon IIIc splicing involves a suboptimal BPS in its native context, it can also repress exon IIIc containing an optimal BPS and a suboptimal PPT. Whereas the branchsite nucleotide and the 3′ splice site YAG clearly play a role in the efficiency of the second step of splicing, the PPT does not appear to influence splicing efficiency after the first step of splicing (26,37,38). Therefore, the fact that either a 'weak' BPS or a 'weak' PPT can facilitate cell-type-specific exon IIIc silencing is further evidence that this regulation does not involve the second step. These findings also lend some insight into the mechanism through which ISE/ISS-3 mediates exon IIIc repression. For example, these results suggest that the mechanism of exon IIIc splicing repression does not interfere with recognition of specific splicing signals, but by more generally preventing exon definition. Exon definition involves cross-exon interactions whereby factors that bind the 5′ and 3′ splice site, often assisted by factors bound at ESE elements, cooperatively facilitate inclusion of the exon. Thus, weak splice sites at either end of an exon can provide an opportunity for additional auxiliary *cis*-elements to assemble complexes that prevent splicing of the exon. Therefore, our results would suggest that while a weak branchpoint is one feature of exon IIIc that presents an opportunity for ISE/ISS-3 to silence its inclusion, other sequence components (e.g. a weak 5′ splice site) that similarly impair the kinetics of spliceosome assembly may also facilitate its silencing. Several combinatorial models have been proposed by which factors bound to exons (ESSs) and introns (ISSs) cooperatively prevent exon definition. In the case of PTB or hnRNPA1, it has been proposed that binding sites on both sides of a regulated exon can repress its inclusion either through protein–protein interactions by proteins bound on both sides of the exon that 'loop out' the exon or create a 'zone of silencing' that sequesters the exon and prevents its splicing (39,40). ESSs within exon IIIc have previously been described that may cooperate with ISE/ISS-3 to assemble a repressor complex that prevents exon IIIc inclusion (18). How the same protein complex assembled on ISE/ISS-3 enhances exon IIIb inclusion will also require further study. While these proteins may directly promote spliceosome assembly on exon IIIb, an alternative model is that they may interfere with factors bound at upstream ISS elements that have previously been shown to otherwise silence exon IIIb exon definition (41). Further characterization of factors that associate with ISE/ISS-3 should allow us to further investigate the mechanisms by which it participates in these dual regulatory activities.

REFERENCES

1. Black,D.L. (2003) Mechanisms of alternative pre-messenger RNA splicing. *Annu. Rev. Biochem.*, **72**, 291–336.
2. Modrek,B. and Lee,C. (2002) A genomic view of alternative splicing. *Nature Genet.*, **30**, 13–19.
3. Johnson,J.M., Castle,J., Garrett-Engele,P., Kan,Z., Loerch,P.M., Armour,C.D., Santos,R., Schadt,E.E., Stoughton,R. and Shoemaker,D.D. (2003) Genome-wide survey of human alternative pre-mRNA splicing with exon junction microarrays. *Science*, **302**, 2141–2144.
4. Matlin,A.J., Clark,F. and Smith,C.W. (2005) Understanding alternative splicing: towards a cellular code. *Nature Rev. Mol. Cell. Biol.*, **6**, 386–398.
5. Moore,M.J., Query,C.C. and Sharp,P.A. (1993) Splicing of precursors to mRNAs by the spliceosome. In Gesteland,R.F. and Atkins,J.F. (eds), *The RNA World.*. Cold Spring Harbor Laboratory, Cold Spring Harbor, pp. 303–358.
6. Zheng,Z.M. (2004) Regulation of alternative RNA splicing by exon definition and exon sequences in viral and mammalian gene expression. *J. Biomed. Sci.*, **11**, 278–294.
7. Ladd,A.N. and Cooper,T.A. (2002) Finding signals that regulate alternative splicing in the post-genomic era. *Genome. Biol.*, **3**, reviews0008.
8. Sorek,R. and Ast,G. (2003) Intronic sequences flanking alternatively spliced exons are conserved between human and mouse. *Genome. Res.*, **13**, 1631–1637.
9. Yeo,G.W., Van Nostrand,E., Holste,D., Poggio,T. and Burge,C.B. (2005) Identification and analysis of alternative splicing events conserved in human and mouse. *Proc. Natl Acad. Sci. USA*, **102**, 2850–2855.
10. Smith,C.W. and Valcarcel,J. (2000) Alternative pre-mRNA splicing: the logic of combinatorial control. *Trends Biochem. Sci.*, **25**, 381–388.
11. Yan,G., Fukabori,Y., McBride,G., Nikolaropolous,S. and McKeehan,W.L. (1993) Exon switching and activation of stromal and embryonic fibroblast growth factor (FGF)-FGF receptor genes in prostate epithelial cells accompany stromal independence and malignancy. *Mol. Cell. Biol.*, **13**, 4513–4522.
12. Carstens,R.P., Eaton,J.V., Krigman,H.R., Walther,P.J. and Garcia-Blanco,M.A. (1997) Alternative splicing of fibroblast growth factor receptor 2 (FGF-R2) in human prostate cancer. *Oncogene*, **15**, 3059–3065.
13. Yasumoto,H., Matsubara,A., Mutaguchi,K., Usui,T. and McKeehan,W.L. (2004) Restoration of fibroblast growth factor receptor2 suppresses growth and tumorigenicity of malignant human prostate carcinoma PC-3 cells. *Prostate*, **61**, 236–242.
14. Carstens,R.P., Wagner,E.J. and Garcia-Blanco,M.A. (2000) An intronic splicing silencer causes skipping of the IIIb exon of fibroblast growth factor receptor 2 through involvement of polypyrimidine tract binding protein. *Mol. Cell. Biol.*, **20**, 7388–7400.
15. Del Gatto-Konczak,F., Bourgeois,C.F., Le Guiner,C., Kister,L., Gesnel,M.C., Stevenin,J. and Breathnach,R. (2000) The RNA-binding protein TIA-1 is a novel mammalian splicing regulator acting through intron sequences adjacent to a 5′ splice site. *Mol. Cell. Biol.*, **20**, 6287–6299.
16. Del Gatto-Konczak,F., Olive,M., Gesnel,M.C. and Breathnach,R. (1999) hnRNP A1 recruited to an exon *in vivo* can function as an exon splicing silencer. *Mol. Cell. Biol.*, **19**, 251–260.
17. Le Guiner,C., Lejeune,F., Galiana,D., Kister,L., Breathnach,R., Stevenin,J. and Del Gatto-Konczak,F. (2001) TIA-1 and TIAR activate splicing of alternative exons with weak 5′ splice sites followed by a U-rich stretch on their own pre-mRNAs. *J. Biol. Chem.*, **276**, 40638–40646.
18. Le Guiner,C., Plet,A., Galiana,D., Gesnel,M.C., Del Gatto-Konczak,F. and Breathnach,R. (2001) Polypyrimidine tract-binding protein represses splicing of a fibroblast growth factor receptor-2 gene alternative exon through exon sequences. *J. Biol. Chem.*, **276**, 43677–43687.
19. Hovhannisyan,R.H. and Carstens,R.P. (2005) A novel intronic *cis* element, ISE/ISS-3, regulates rat fibroblast growth factor receptor 2 splicing through activation of an upstream exon and repression of a downstream exon containing a noncanonical branch point sequence. *Mol. Cell. Biol.*, **25**, 250–263.
20. Carstens,R.P., McKeehan,W.L. and Garcia-Blanco,M.A. (1998) An intronic sequence element mediates both activation and repression of rat fibroblast growth factor receptor 2 pre-mRNA splicing. *Mol. Cell. Biol.*, **18**, 2205–2217.
21. Dignam,J.D., Lebovitz,R.M. and Roeder,R.G. (1983) Accurate transcription initiation by RNA polymerase II in a soluble extract from isolated mammalian nuclei. *Nucleic Acids Res.*, **11**, 1475–1489.
22. Muh,S.J., Hovhannisyan,R.H. and Carstens,R.P. (2002) A Non-sequence-specific double-stranded RNA structural element regulates splicing of two mutually exclusive exons of fibroblast growth factor receptor 2 (FGFR2). *J. Biol. Chem.*, **277**, 50143–50154.
23. Baraniak,A.P., Lasda,E.L., Wagner,E.J. and Garcia-Blanco,M.A. (2003) A stem structure in fibroblast growth factor receptor 2 transcripts mediates cell-type-specific splicing by approximating intronic control elements. *Mol. Cell. Biol.*, **23**, 9327–9337.
24. Query,C.C., Strobel,S.A. and Sharp,P.A. (1996) Three recognition events at the branch-site adenine. *EMBO J.*, **15**, 1392–1402.
25. Sekiguchi,M., Sakakibara,K. and Fujii,G. (1978) Establishment of cultured cell lines derived from a human gastric carcinoma. *Jpn. J. Exp. Med.*, **48**, 61–68.
26. Coolidge,C.J., Seely,R.J. and Patton,J.G. (1997) Functional analysis of the polypyrimidine tract in pre-mRNA splicing. *Nucleic Acids Res.*, **25**, 888–896.
27. Roscigno,R.F., Weiner,M. and Garcia-Blanco,M.A. (1993) A mutational analysis of the polypyrimidine tract of introns. Effects of sequence differences in pyrimidine tracts on splicing. *J. Biol. Chem.*, **268**, 11222–11229.
28. Buvoli,M., Mayer,S.A. and Patton,J.G. (1997) Functional crosstalk between exon enhancers, polypyrimidine tracts and branchpoint sequences. *EMBO J.*, **16**, 7174–7183.
29. Han,J. and Cooper,T.A. (2005) Identification of CELF splicing activation and repression domains *in vivo*. *Nucleic Acids Res.*, **33**, 2769–2780.
30. Dredge,B.K., Stefani,G., Engelhard,C.C. and Darnell,R.B. (2005) Nova autoregulation reveals dual functions in neuronal splicing. *EMBO J.*, **24**, 1608–1620.
31. Zhang,W., Liu,H., Han,K. and Grabowski,P.J. (2002) Region-specific alternative splicing in the nervous system: implications for regulation by the RNA-binding protein NAPOR. *RNA*, **8**, 671–685.
32. Kanopka,A., Muhlemann,O. and Akusjarvi,G. (1996) Inhibition by SR proteins of splicing of a regulated adenovirus pre-mRNA. *Nature*, **381**, 535–538.
33. Jin,Y., Suzuki,H., Maegawa,S., Endo,H., Sugano,S., Hashimoto,K., Yasuda,K. and Inoue,K. (2003) A vertebrate RNA-binding protein Fox-1 regulates tissue-specific splicing via the pentanucleotide GCAUG. *EMBO J.*, **22**, 905–912.
34. Hui,J., Hung,L.H., Heiner,M., Schreiner,S., Neumuller,N., Reither,G., Haas,S.A. and Bindereif,A. (2005) Intronic CA-repeat and CA-rich elements: a new class of regulators of mammalian alternative splicing. *EMBO J.*, **24**, 1988–1998.
35. Wang,Z., Rolish,M.E., Yeo,G., Tung,V., Mawson,M. and Burge,C.B. (2004) Systematic identification and analysis of exonic splicing silencers. *Cell*, **119**, 831–845.
36. Lallena,M.J., Chalmers,K.J., Llamazares,S., Lamond,A.I. and Valcarcel,J. (2002) Splicing regulation at the second catalytic step by Sex-lethal involves 3′ splice site recognition by SPF45. *Cell*, **109**, 285–296.
37. Anderson,K. and Moore,M.J. (1997) Bimolecular exon ligation by the human spliceosome. *Science*, **276**, 1712–1716.
38. Bennett,M., Michaud,S., Kingston,J. and Reed,R. (1992) Protein components specifically associated with prespliceosome and spliceosome complexes. *Genes Dev.*, **6**, 1986–2000.
39. Blanchette,M. and Chabot,B. (1999) Modulation of exon skipping by high-affinity hnRNP A1-binding sites and by intron elements that repress splice site utilization. *EMBO J.*, **18**, 1939–1952.
40. Wagner,E.J. and Garcia-Blanco,M.A. (2001) Polypyrimidine tract binding protein antagonizes exon definition. *Mol. Cell. Biol.*, **21**, 3281–3288.
41. Wagner,E.J., Baraniak,A.P., Sessions,O.M., Mauger,D., Moskowitz,E. and Garcia-Blanco,M.A. (2005) Characterization of the intronic splicing silencers flanking FGFR2 exon IIIb. *J. Biol. Chem.*, **280**, 14017–14027.